

Investigating the Effect of Some Train and Track Parameters on Contact-impact Forces in the Vicinity of a Rail Breakage

Mosab Reza Tajalli¹, Jabbar Ali Zakeri^{1*}

¹ Department of Railway Track & Structures Engineering, Faculty of Railway Engineering, Iran University of Science and Technology, Narmak, Teheran, Iran, 1684613114

* Corresponding author, e-mail: zakeri@iust.ac.ir

Received: 03 September 2018, Accepted: 15 July 2019, Published online: 24 September 2019

Abstract

Broken rails or welds are the main causes of derailment in railway networks. Therefore, a wheel-rail interaction model, which precisely estimates contact-impact forces in the presence of broken rails, can have a significant effect on derailment risk reduction. This paper attempts to present contact-impact forces in the vicinity of broken rails by employing a detailed 3D finite element model. The model is verified using a field test carried out on a ballasted railway track. Effects of train speed, gap length, axle load and railpad and ballast characteristics are studied on rail-wheel contact forces as well as on railpad and ballast forces. Results suggest that increasing the train speed from 60 km/h to 110 km/h would increase dynamic impact force from 2.46 to 4.11. It is also observed that increasing axle load results in an increase in the wheel-rail impact forces and in railpad and ballast forces, while leading to a reduced dynamic impact factor. Furthermore, investigating the effect of the track parameters demonstrates that ballast stiffness is the most important characteristic of the track, which has a reverse effect on dynamic impact forces. Moreover, unloading length increase and consequently derailment risk increase is highly sensitive to increasing train speed.

Keywords

wheel-rail interaction, contact-impact force, rail breakage, finite element, dynamic analysis

1 Introduction

Recently, there has been an ever-increasing rail transport demand. To deal with such a demand, railway organizations have employed various approaches such as increasing the operational speed and axle loads of their railway networks. Doing so has led to an increasing pressure on infrastructures and a greater necessity for a better understanding of the structural behavior of track elements. In this regard, researches have studied track elements and parameters affecting them as well as various methods for optimization of each element [1, 2]. Furthermore, some statistical studies show that increased pressure on rails leads to increased number of broken rails or welds in railway networks per year, which is the main cause of train derailment [3–5]. In this regard, investigation of influence of track parameters on contact forces is crucial to derailment risk reduction in the vicinity of a broken rail.

The wheel-rail interaction in the vicinity of the rail breakage is to some extent similar to a wheel passing similar discontinuities in the rail, such as expansion joints, insulated rail joints, switches, etc. Due to the complex interaction

of wheels and rails, it is not possible to employ a single point Hertz spring in a continuous manner to simulate the interaction of wheels and rails. Steenbergen [6] studied a moving vehicle over rail discontinuities by employing a continuous-single-point contact model and a transient double-point contact model. In the first model, the discontinuity of the rail was introduced as an irregularity function in the interaction model. However, in the second model, the initial speed in vertical direction was also included. It was concluded that employing the first model led to an underestimation of the wheel-rail contact forces.

Jenkins et al. [7] studied the dipped joint using a rigid body dynamic method. To model the contact of wheels and rails, a non-linear Hertz spring was used. Results suggested that two impact forces of P1 (almost 5–6 times larger than the static force of the wheel) and P2 (almost 3–4 times larger than the static force of the wheel) were produced.

Wu and Thompson [8] studied the effects of rail joints on impact forces and emitted noise. They modeled a train as an unsprung mass, a track as two infinite beams resting

on a spring-mass-spring (railpad stiffness, traverse mass, ballast stiffness) and the wheel-rail interaction using non-linear Hertz springs. Rail joints are introduced in interaction equations as an irregularity function. They also studied effects of gap length, vertical misalignment and dipped rail on a joint. It was shown that impact forces could be 4–6 times larger than static wheel loads.

Employing 3D finite element models for studying the wheel-rail interaction has gained significant attention during recent years due to development of numerical methods and efficiency of computers [9–13]. Mandal et al. [14] studied wheel impacts generated by passing over dipped rail joints. They employed a 3D model of the train-track interaction to investigate impact forces and compare them with field-measured data. Moreover, they presented non-dimensional equations to determine P1 and P2 impact forces, which could be used as lower limit predictors. Although many researches have studied impacts of wheel crossing short wave length irregularities and discontinuities such as rail joints and switches, less attention has been paid to effects of the rail breakage on the dynamic interaction of track and trains.

Gonzalez et al. [15] studied the safety of underground vehicles in highly resilient tracks, where the rail breakage occurred. A multibody system with discrete mass and springs was employed to model a train, and the track was modeled with finite elements. The model produced similar responses for various tracks with a maximum speed of 110 km/h. As the speed decreased, the safety index was reduced for the tracks. In another study, derailment probability was investigated with the assumption of the rail breakage in the curved section of the track [16]. Moreover, effects of the rail breakage in interior/exterior rails, sleeper spacing, and position of the rail breakage were studied. Results suggested that the Nadal derailment index and the unloading index never exceeded allowable thresholds. Moreover, it was concluded that the unloading index was more critical compared to the Nadal index. It was also shown that the rail breakage was more critical in exterior rails than in interior rails. The rail breakage on a sleeper resulted in a higher derailment index compared to the rail breakage between two adjacent sleepers.

Some researchers have studied contact-impact forces using field tests [17, 18]. Askarnejad et al. [19] carried out a field test on insulated rail joints to investigate the dynamic response of the track. They concluded that reduction of sleeper spacing adjacent to the gap could decrease acceleration values of sleepers and ballast pressure.

The aim of this paper is to investigate the effect of train and track characteristics on contact-impact forces in the vicinity of the rail breakage by 3D finite element modeling. Moreover, investigation of railpad and ballast dynamic forces, which are important elements in the track superstructure, and contribute largely to the costs of maintenance, is another purpose of this study. An accurate study of railpad and ballast forces can produce more accurate results to assess life-cycle costs in similar rail discontinuities and short wave length irregularities, such as corrugations, insulated rail joints and crossings. Numerical model verification is carried out by comparing numerical results with experimental results measured in a field test.

2 Finite element modeling

As shown in Fig. 1, the rail on the discrete support model has been employed to investigate the dynamic response of the track. In this regard, a finite element model has been created in several steps using the ABAQUS FE package [20]. Firstly, part module tools have been used to model the geometry of track elements and wheels. Main structural elements of ballasted tracks include rails, railpads, fasteners, sleepers, ballast and substructure. Considering the aim of modeling and effect of each element on results, some of these elements are considered in the model. In the dynamic rail-wheel interaction by short wave length irregularities, the rail is the most important element of the track.

In this study, the rail, like the wheel part, is modeled by solid elements in the contact region to assess accurate impact forces in the vicinity of the rail breakage. Fig. 2 presents the geometrical profile of UIC60 rails and the modeled profile. The rail is modeled by beam elements in the region far from the gap to reduce computational effort. The study shows that a total length of 13.6 m is needed for the load influence length considering the bending and reverse bending of the rail in the both sides of the rail breakage.

Secondly, the material characteristics of wheel and rail steel are defined and assigned in the property module. Because of impact forces in the vicinity of the broken rail and extremely high stresses, constitutive behavior of the steel material is chosen with the elasto-plastic model in this region. However, in other regions, the material is modeled with the elastic behavior model. Elastic properties of steel have been defined in the model, as presented in Table 1. Moreover, plastic properties of steel have been defined, as listed in Table 2 [21].

Table 1 The physical characteristics of the model

Track Model Parameters	values
Steel modulus of elasticity	210 GPa
Steel Poisson's ratio	0.3
Steel Density	7850 kg/m ³
Railpad stiffness	250 × 103 kN/m
Railpad damping	250 kNs/m
Sleeper mass	160 kg
Ballast stiffness	70 × 103 kN/m
Ballast damping	180 kNs/m
Ballast mass	1400 kg
Substructure stiffness	130 × 103 kN/m
Substructure damping	62.3 kNs/m

Table 2 The plastic properties of steel

Stress (Mpa)	Plastic strain
830	0
1230	0.01
1240	0.1

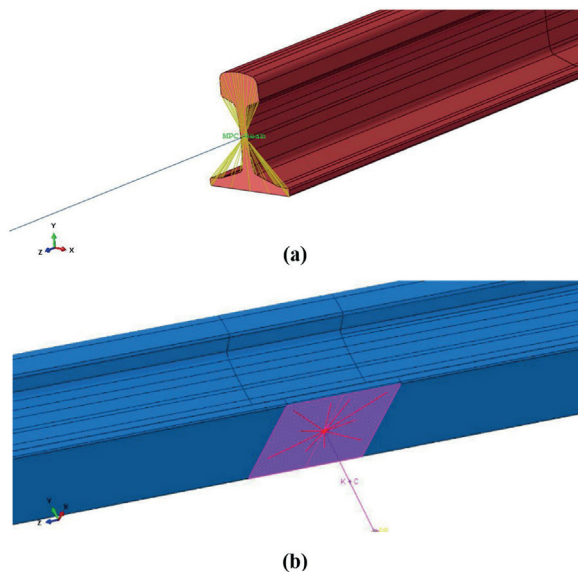


Fig. 3 The modeling technics: (a) connecting the beam and solid elements with MPC; (b) modeling the boundary condition of the rail support on sleepers by coupling

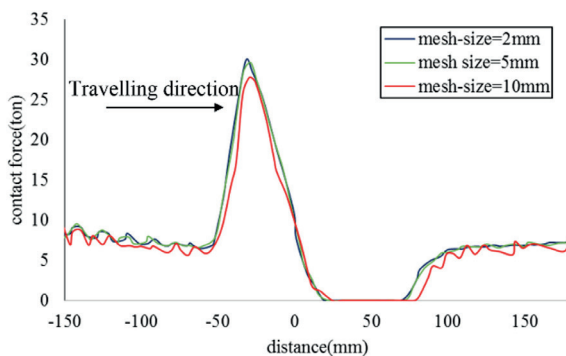


Fig. 4 Contact force history curves with different mesh sizes

3 Model verification

Generally, rail-wheel contact forces are measured in field tests using three major methods. The first method is based on wheel instrumentation and needs special softwares, which require high technology and cost. The acceleration measurement of the rail heel in a track region and an inverse approach are used to estimate contact forces in the second method, which does not yield accurate results in contact-impact problems [22]. The third method, which is used in this study, is based on the Wheatstone bridge circuit.

When the wheel crosses over rail discontinuity, it strikes the rail head and introduces a shear force in the rail section, which could be measured by a strain bridge set-up on the rail web. According to these equations, the shear force is as a function of shear strain values.

$$\varepsilon_1 = \frac{VQ}{2GI_x t} + \frac{T}{2GJ} + \frac{M_y t}{4EI_y} \quad (1)$$

$$\varepsilon_2 = -\frac{VQ}{2GI_x t} - \frac{T}{2GJ} + \frac{M_y t}{4EI_y} \quad (2)$$

$$\varepsilon_3 = \frac{VQ}{2GI_x t} - \frac{T}{2GJ} - \frac{M_y t}{4EI_y} \quad (3)$$

$$\varepsilon_4 = -\frac{VQ}{2GI_x t} + \frac{T}{2GJ} - \frac{M_y t}{4EI_y} \quad (4)$$

$$V = \frac{1}{2Q} [GI_x t [(\varepsilon_1 + \varepsilon_3) - (\varepsilon_2 + \varepsilon_4)]] \quad (5)$$

where ε_i are shear strains at neutral axis level in 45-degree directions in the both sides of the rail web (Fig. 5), I_x and I_y are the moments of inertia of the rail related to x-axis and y-axis, respectively, t is the thickness of the rail web, Q is the static moment of the rail section area, E is the modulus of elasticity, G is the shear modulus, J is the torsional modulus of the rail, V is the shear force in the rail section due to impact force, M_y is the bending moment in the section related to y-axis, and T is the torque in the rail section.

As shown in Fig. 5, there is no pad/ballast reaction force in the vicinity of the free end of the rail, and therefore, the measured shear value in this section according to the Eq. (1) to Eq. (5) is equal to wheel/rail contact-impact forces.

In order to measure the rail-wheel impact force, one of the railway station tracks in Tehran is chosen and it is instrumented in the vicinity of a rail joint. Fishplates are separated to make a rail discontinuity and a strain bridge is installed in the rail web, as shown in Fig. 6. A single

locomotive with the axle load of 21 tons is used for the test train. The axle spacing of a bogie and bogie center spacing are 2.7 m and 12.5 m, respectively.

A dynamic test is carried out on the site, in which the test train passes with the speed of 30 km/h. The shear force is recorded with the shear strain bridge set up as the wheel passes over rail discontinuity and strikes the rail head. According to the previous section, a numerical model is used and it is verified with the test results. The rail modulus is determined equal to 20.4 Mpa using the Talbot method [23], which is used in discrete spring stiffness.

Fig. 7 presents the comparison of numerical and experimental results. The test results show that the maximum impact force is 14.3 tons, which is 1.36 times greater than the static wheel load. As clearly observed, numerical results have an acceptable agreement with experimental results [Fig. 7(b)].

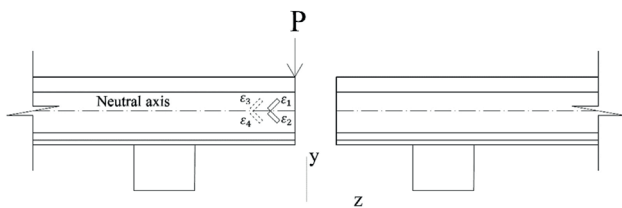


Fig. 5 The schematic view of strain bridge instrumentation

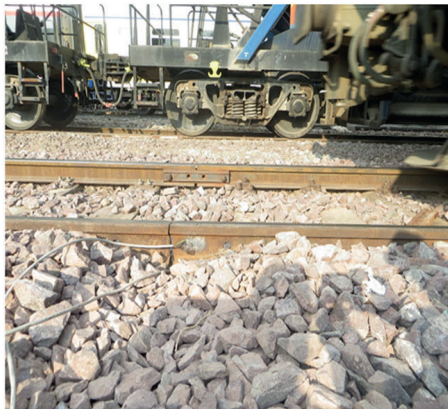


Fig. 6 The overview of the track, locomotive and rail instrumentation

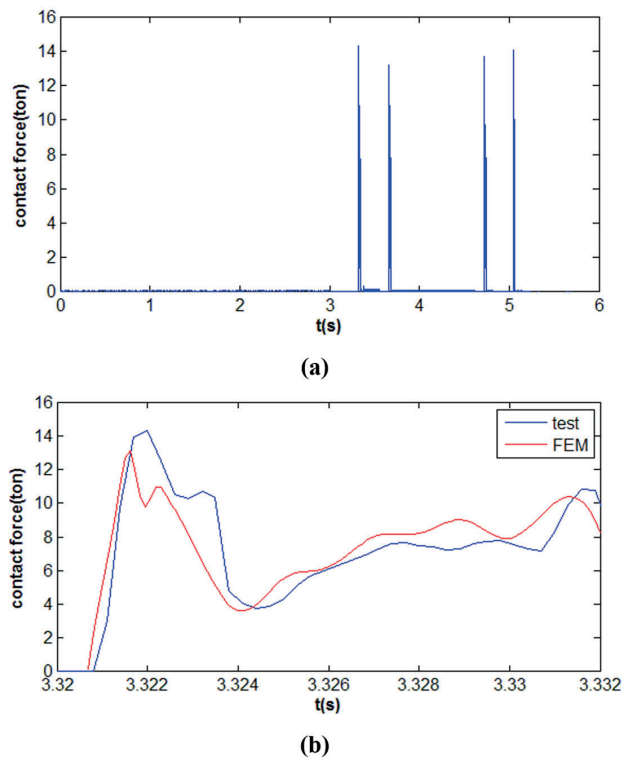


Fig. 7 The overview of the track, locomotive and rail instrumentation

4 Commentary on results

4.1 Effects of speed

In order to study the effects of speed on the dynamic response of the track, dynamic analyses are carried out for speeds varying from 60 km/h to 110 km/h, increasing in steps of 10 km/h. Fig. 8(a) presents the effects of speed on the wheel-rail contact force curve. These curves show the time history of the contact force between the wheel and the rail as the wheel rolls over the rail. To make a good comparison of curves, the horizontal axis represents the relative distance of the wheel center from the rail break-age location.

According to the results, unloading length, in which the contact force is zero, has increased by increasing the train speed, which is the main cause of train derailment in straight tracks. The derailment index is calculated based on the ratio of lateral to vertical wheel load. The threshold for this value varies in different standards, from 0.6 to 1.0 [24]. Moreover, in some of the standards, it is stated that derailment occurs only when the derailment index is exceeded for a specific amount of time/distance. Moreover, the time when the contact between the wheel and the rail is lost and the contact force is zero is added to the time when the derailment index exceeds its threshold [25]. As a result, higher time/distance of unloading leads to higher derailment probability.

Since the static wheel load is 10 tons, the dynamic impact factor (DIF) is defined as the maximum contact force to the wheel static force. Results suggest that DIF is 2.46 at a speed of 60 km/h, while it is 4.11 at a speed of 110 km/h.

Static analysis shows that the force is 4.9 tons in the railpad and the ballast in the vicinity of the rail breakage. As shown in Fig. 8(b), dynamic analyses suggest that forces in the railpad, due to the impact exerted on the rail at speeds of 60 and 110 km/h, are 16.4 and 31.9 tons, which are 3.4 and 6.6 times larger than the railpad force at static analysis, respectively. Moreover, dynamic forces in the ballast, due to the impact exerted on the rail in the minimum and maximum train speeds, are 8.8 and 13.6 tons, which are 1.8 and 2.8 times larger than the ballast force at static analysis, respectively. Results suggest that increasing speed almost linearly increases wheel-rail, railpad, and ballast impact forces. Moreover, the increasing rate of railpad forces is almost the same as increasing wheel-rail forces, although the increasing rate of ballast forces is significantly lower than them.

4.2 Effects of wheel load

Today, there is a growing need for higher traffic which requires the passage of higher axle loads in railway networks. To study the effects of wheel load on the dynamic response of the track, dynamic analyses are carried out for

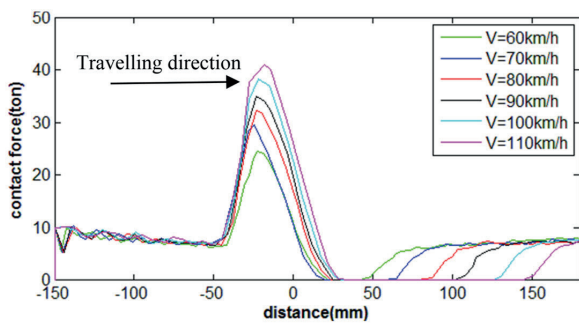
wheel loads of 7.5, 10, 12.5, and 15 tons. The results illustrated in Fig. 9 show that the maximum impact is 22.6 tons for a wheel load of 7.5 tons, while it is 37.4 tons for a wheel load of 15 tons. Corresponding DIF values for wheel loads of 7.5 and 15 tons are 3.0 and 2.5, suggesting that as wheel load increases, the DIF value decreases. Moreover, increasing wheel load does not cause significant changes in unloading length and consequently in derailment risk.

As shown in Fig. 9(b), forces in the railpad, due to forces exerted on the rails for wheel loads of 7.5 and 15 tons, are 16.8 and 26.1 tons, which are 4.6 and 5.6 times larger than static forces, respectively. Moreover, results suggest that forces in the ballast for the minimum and maximum value of the considered wheel load are 8.1 and 12.7 tons, which are 2.2 and 1.7 times larger than static forces, respectively.

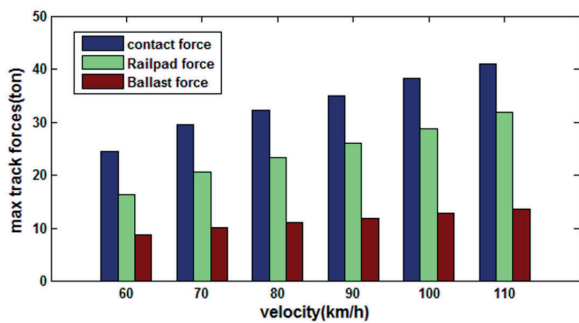
4.3 Effects of ballast characteristics

To study the effects of ballast characteristics on the track dynamic response, dynamic analyses are carried out for ballast stiffness values of 20, 70, and 120 MN/m and damping values of 30, 80, 130, and 180 kNs/m at a speed of 70 km/h. Fig. 10 presents the effect of ballast characteristics on maximum values of track forces.

Results suggest that by increasing the ballast damping value from 30 kNs/m to 180 kNs/m, the maximum impact force increases from 28.6 tons to 29.6 tons. Moreover,

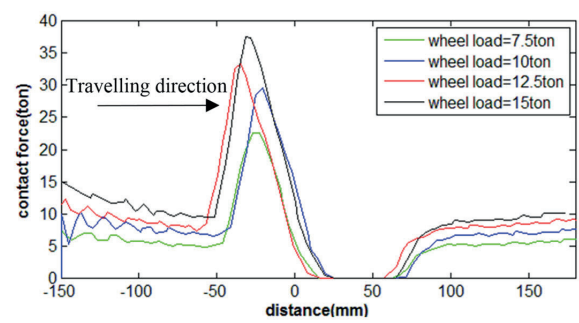


(a)

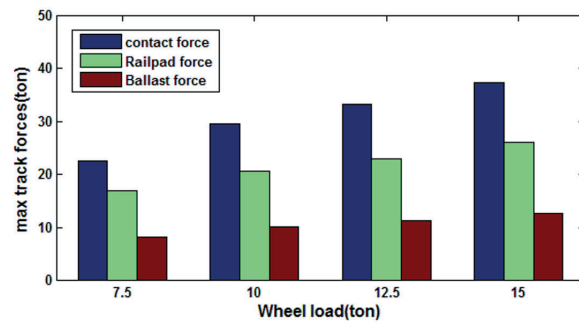


(b)

Fig. 8 Effects of speed on (a) contact force signature and (b) maximum track forces



(a)



(b)

Fig. 9 Effects of wheel load on (a) contact force signature and (b) maximum track forces

ballast stiffness has a reverse impact on the impact factor. Increasing ballast stiffness from 20 MN/m to 120 MN/m would reduce maximum impact forces from 36.7 tons to 26.8 tons. By reducing ballast stiffness, the cantilever rail deflection would increase that might lead to an increase in the impact force.

Results suggest that increasing the ballast damping value in the considered range does not cause a significant change in railpad forces as it does not cause an increase in wheel-rail impact forces; this increase is about 5 %. Noticeable changes also occur with regard to ballast forces. An increase of ballast damping will cause an increase of 36 % in maximum ballast forces. Moreover, as shown in Fig. 10(b), increasing the ballast stiffness value from 20 MN/m to 120 MN/m reduces maximum impact forces in the railpad and ballast from 28.5 tons to 18.5 tons and 12.5 tons to 10.4 tons, respectively.

4.4 Effects of railpad characteristics

To study effects of railpad characteristics on the dynamic response of the track, dynamic analyses are carried out for railpad stiffness values of 50, 250, and 500 MN/m and railpad damping values of 50, 250, and 500 kNs/m at a speed of 70 km/h.

As shown in Fig. 11(a), although increasing the railpad damping value from 50 kNs/m to 500 kNs/m increases

the maximum impact force from 28.6 tons to 34.3 tons, it remains roughly unchanged by increasing railpad stiffness in the considered range [Fig. 11(b)].

Results suggest that increasing the railpad damping value increases maximum forces in the railpad from 15.9 tons to 22.7 tons. However, increasing railpad stiffness does not have any significant effect on railpad forces. Moreover, increasing railpad damping and stiffness increases maximum forces exerted on the ballast by 11 % and 19 %, respectively.

4.5 Effects of gap length

The gap between rails is one of the factors, which increases the rate of rail deterioration. In such instances, the impact of the wheel as it crosses over the free end of the rail could cause significant stresses in the rail. Mandal studied the railhead damage of gapped rail joints and showed that as the rail gap increased, the residual deformations and plastic strains in the rail increased as well, which resulted in a higher probability of material deterioration [26].

To study the effects of gap length on the dynamic response of the track, dynamic analyses are carried out for gap lengths of 5, 15, 25, and 35 mm. Fig. 12(a) presents the effects of gap length on the time-history of wheel-rail contact forces at different gap lengths. Moreover, Fig. 12(b) shows the effects of gap length on the maximum contact

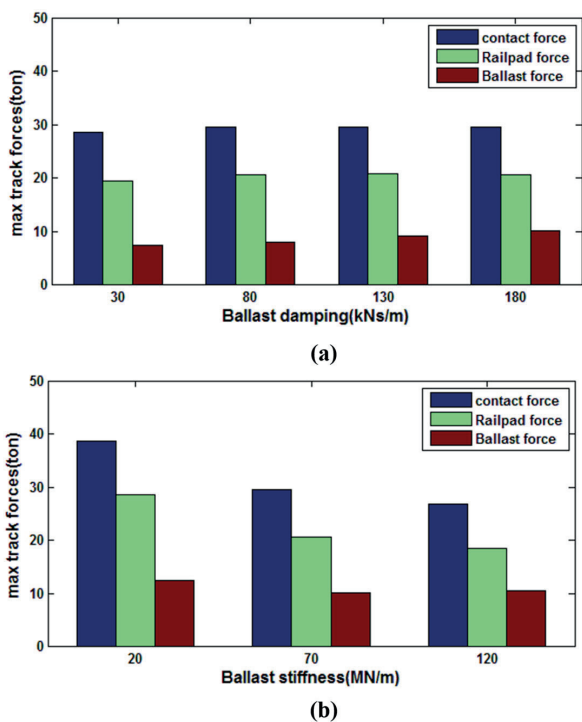


Fig. 10 The maximum values of track forces at different values of (a) ballast damping and (b) ballast stiffness

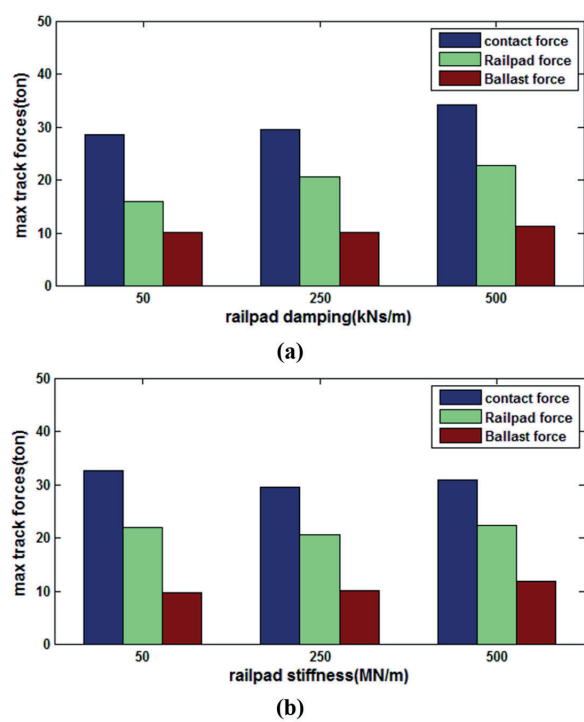


Fig. 11 The maximum values of track forces at different values of (a) railpad damping and (b) railpad stiffness

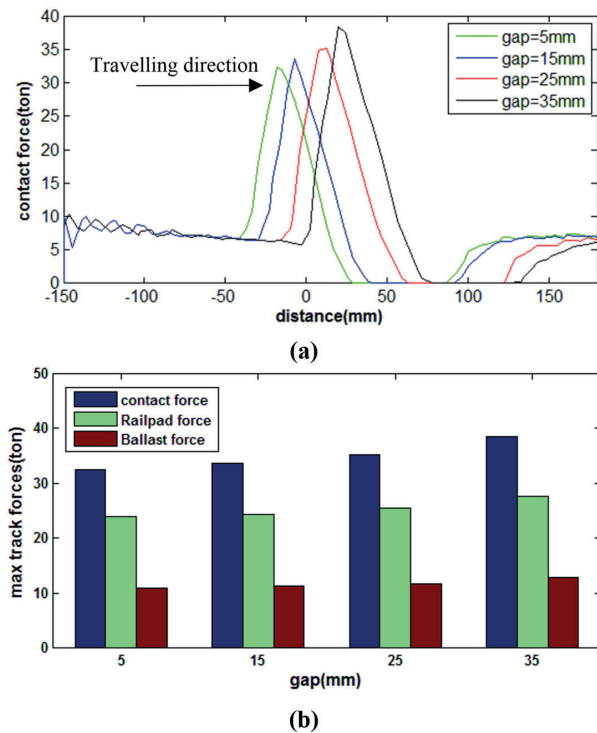


Fig. 12 The maximum values of track forces at different values of (a) railpad damping and (b) railpad stiffness

forces of the wheel as it crosses the rail breakage and also on forces exerted on the railpad and ballast. According to the results, increasing gap length from 5 mm to 35 mm increases wheel-rail contact forces by 18 %. The results suggest that DIF is 3.24 for a gap length of 5 mm, while it is 3.84 for a gap length of 35 mm.

5 Conclusions

Finite element modeling of the wheel-rail interaction is employed to study the effects of speed, wheel load, gap length, and railpad and ballast characteristics on impact forces in the vicinity of the rail breakage. The track model has been composed of fasteners, railpads, ballast and sub-structure, which have been modeled as a combination of masses, springs and dampers and the rail which is modeled by solid elements in the contact region and by beam elements in others. Moreover, the wheel has been modeled by solid elements, and the wheel and rail materials have

nonlinear behavior in the contact surface. A field test has been carried out by passing a locomotive over a rail discontinuity, which is made by separating fishplates at a rail joint. A summary of field measurements and numerical results is as follows:

According to the field test results at the speed of 30 km/h, the maximum impact force is 14.3 tons and the dynamic impact factor is 1.36. Comparing the experimental results with the numerical results shows that the finite element model could have a real estimation of contact-impact forces. The difference in areas under experimental and numerical curves is less than 18 %.

Increasing speed linearly increases track forces, but the increasing rate of ballast impact forces is less than that of wheel-rail and railpad forces. DIFs for minimum and maximum train speeds are 2.46 and 4.11, respectively. Furthermore, unloading length increases by increasing speed, which leads to an increasing risk of derailment.

Although increasing wheel load increases wheel-rail, railpad and ballast impact forces, it decreases DIF values. DIFs for wheel loads of 7.5 and 15 tons are 3 and 2.5, respectively. Moreover, by increasing wheel load, both railpad forces and ballast forces increase by about 55 % for the considered range of axle load.

Studying the ballast characteristics effect shows that ballast damping does not have any significant effect on wheel-rail and railpad forces. However, an increase in ballast damping from 30 kNs/m to 180 kNs/m causes an increase of 36 % in the maximum ballast force. Moreover, increasing ballast stiffness results in reduced track forces. Studying effects of railpad characteristics shows that noticeable changes occur with regard to contact forces and railpad forces by increasing railpad damping in the considered range. Additionally, results show that increasing railpad stiffness does not have any significant effect on wheel-rail and railpad forces, but it causes a perceptible change in ballast forces.

Increasing gap length increases wheel-rail, railpad, and ballast impact forces; however, the increment of forces is rather small. Moreover, increasing gap length from 5 to 35 mm increases wheel-rail contact forces by 18 %.

References

- [1] Cai, Z., Raymond, G. P. "Modelling the dynamic response of railway track to wheel/rail impact loading", *Structural Engineering and Mechanics*, 2(1), pp. 95–112, 1994. <https://doi.org/10.12989/sem.1994.2.1.095>
- [2] Mosayebi, S. A., Zakeri, J. A., Esmaili, M., "Some aspects of support stiffness effects on dynamic ballasted railway tracks", *Periodica Polytechnica Civil Engineering*, 60(3), pp. 427–436, 2016. <https://doi.org/10.3311/PPci.7933>

- [2] Zakeri, J. A. "Statistical Analysis of Rail Breakage and Rail Welding Failures in Iranian Railways", presented at CD-Proceedings of the 7th international Conference on Railway Engineering, London, UK, June 29–30, 2005.
- [3] Sawley, K., Reiff, R. "An assessment of Railtrack's methods for managing broken and defective rails", Office of the Rail Regulator, Transportation Technology Center, Inc. A subsidiary of the Association of American Railroads Pueblo, CO, USA, 2000.
- [4] Liu, X., Saat, M. R., Barkan, C. P. L. "Analysis of Causes of Major Train Derailment and Their Effect on Accident Rates", Journal of the Transportation Research Board, 2289(1), pp. 154–163, 2012.
<https://doi.org/10.3141/2289-20>
- [5] Steenbergen, M. J. M. M. "Modelling of wheels and rail discontinuities in dynamic wheel-rail contact analysis", Vehicle System Dynamics, 44(10), pp. 763–787, 2007.
<https://doi.org/10.1080/00423110600648535>
- [6] Jenkins, H. H., Stephenson, J. E., Clayton, G. A., Morland, G. W., Lyon, D. "The effect of track and vehicle parameters on wheel/rail vertical dynamic forces", Railway Engineering Journal, 3(1), pp. 2–16, 1974.
- [7] Wu, T. X., Thompson, D. J. "On the impact noise generation due to a wheel passing over rail joints", Journal of Sound and Vibration, 267(3), pp. 485–496, 2003.
[https://doi.org/10.1016/S0022-460X\(03\)00709-0](https://doi.org/10.1016/S0022-460X(03)00709-0)
- [8] Wiest, M., Daves, W., Fischer, F. D., Ossberger, H. "Deformation and damage of a crossing nose due to wheel passages", Wear, 265(9–10), pp. 1431–1438, 2008.
<https://doi.org/10.1016/j.wear.2008.01.033>
- [9] Wen, Z., Jin, X., Zhang, W. "Contact-impact stress analysis of rail joint region using the dynamic finite element method", Wear, 258(7–8), pp. 1301–1309, 2005.
<https://doi.org/10.1016/j.wear.2004.03.040>
- [10] Li, Z., Zhao, X., Esveld, C., Dollevoet, R., Molodova, M. "An investigation into the Causes of squats – Correlation analysis and numerical modelling", Wear, 265(9–10), pp. 1349–1355, 2008.
<https://doi.org/10.1016/j.wear.2008.02.037>
- [11] Oregui, M., Li, Z., Dollevoet, R. P. B. J. "An investigation into the relation between wheel/rail contact and bolt tightness of rail joints using a dynamic finite element model", In: Proceedings of the 9th International Conference on Contact Mechanics and Wear of Rail/Wheel Systems, Chengdu, China, 2012, pp. 501–508.
- [12] Mandal, N. K., Peach, B. "An Engineering Analysis of Insulated Rail Joints: A General Perspective", International Journal of Engineering Science and Technology, 2(8), pp. 3964–3988, 2010. [online] Available at: https://www.researchgate.net/publication/50346113_An_Engineering_Analysis_of_Insulated_Rail_Joints_A_General_Perspective [Accessed: 10 July 2019]
- [13] Mandal, N. K., Dhanasekar, M., Sun, Y. Q. "Impact forces at dipped rail joints", Journal of Rail and Rapid Transit, 230(1), pp. 271–282, 2016.
<https://doi.org/10.1177/0954409714537816>
- [14] Gonzalez, F. J., Suarez, B., Paulin, J., Fernandez, I. "Safety assessment of underground vehicles passing over highly resilient straight track in the presence of a broken rail", Journal of Rail and Rapid Transit, 222(1), pp. 69–84, 2008.
<https://doi.org/10.1243/09544097JRRT128>
- [14] Suárez, B., Rodriguez, P., Vázquez, M., Fernández, I. "Safety assessment of underground vehicles passing over highly resilient curved tracks in the presence of a broken rail", Vehicle System Dynamics, 50(1), pp. 59–78, 2011.
<https://doi.org/10.1080/00423114.2011.563859>
- [15] Ataei, S., Mohammadzadeh, S., Miri, A. "Dynamic forces at square and inclined rail joints: field experiments", Journal of Transportation Engineering, 142(9), 2016.
[https://doi.org/10.1061/\(ASCE\)TE.1943-5436.0000866](https://doi.org/10.1061/(ASCE)TE.1943-5436.0000866)
- [16] Gullers, P., Andersson, L., Lundén, R. "High-frequency vertical wheel-rail contact forces – Field measurements and influence of track irregularities", Wear, 265(9–10), pp. 1472–1478, 2008.
<https://doi.org/10.1016/j.wear.2008.02.035>
- [17] Askarinejad, H., Dhanasekar, M., Colin, C. "Assessing the effects of track input on the response of insulated rail joints using field experiments", Journal of Rail and Rapid Transit, 227(2), pp. 176–187, 2013.
<https://doi.org/10.1177/0954409712458496>
- [18] ABAQUS "User's Manual, (6.4)", [computer program] Available at: <https://www.3ds.com/products-services/simulia/products/abaqus/> [Accessed: 10 July 2019]
- [19] Pang, T., Dhanasekar, M. "Dynamic finite element analysis of the wheel–rail interaction adjacent to the insulated rail joints", In: Proceedings of the 7th International Conference on Contact Mechanics and Wear of Wheel/Rail Systems, Brisbane, Australia, 2006, pp. 509–516.
- [20] Johansson, A., Nielsen, J. C. O. "Out-of-round railway wheels – wheel-rail contact forces and track response derived from field tests and numerical simulations", Journal of Rail and Rapid Transit, 217(2), pp. 135–146, 2003.
<https://doi.org/10.1243/095440903765762878>
- [21] Talbot, A. N. "Stresses in Railroad Track, Report of the Special Committee on Stresses in Railroad Track", Proceeding of the AREA, First progress report, 19, pp. 73–1062, 1918.
- [22] Younesian, D., Abedi, M., Hazrati Ashtiani, I. "Dynamic analysis of a partially filled tanker train travelling on a curved track", International Journal of Heavy Vehicle Systems, 17(3/4), pp. 331–358, 2010.
<https://doi.org/10.1504/IJHVS.2010.035993>
- [23] Ishida, H., Matsuo, M., Fujioka, T. "Safety Assessment Method of Railway Vehicle under Oscillatory Wheel Load Fluctuation", Journal of Environment and Engineering, 2(2), pp. 407–418, 2007.
<https://doi.org/10.1299/jee.2.407>
- [24] Mandal, N. K. "Ratcheting damage of railhead material of gapped rail joints with reference to free end effects", Journal of Rail and Rapid Transit, 231(2), pp. 211–225, 2017.
<https://doi.org/10.1177/0954409715625361>